https://doi.org/10.5194/hess-2022-243
Preprint. Discussion started: 28 July 2022

Hydrology and Earth System Sciences
Discussions

Widespread flooding dynamics changing under climate change: characterising floods using UKCP18

Adam Griffin[1], Alison Kay[1], Paul Sayers[2], Victoria Bell[1], Elizabeth Stewart[1], Sam Carr[2]
[1]UK Centre for Ecology & Hydrology, Wallingford, Oxfordshire, OX10 8BB, UK.
[2]Sayers and Partners, Watlington, Oxfordshire, OX49 5PY, UK.

Correspondence to: Adam Griffin (adagri@ceh.ac.uk)

Abstract. An event-based approach has been used to explore the potential effects of climate change on the spatial and temporal coherence of widespread flood events in Great Britain. Time series of daily mean river flow were generated using a gridded national-scale hydrological model (Grid-to-Grid) driven by the 12-member ensemble of regional climate projections from UKCP18. Gridded flow series were generated nationally for 30-year baseline (1980-2010) and future (2051-2080) time-slices from which sets of widespread extreme events were extracted. These events were defined as exceeding an at-site 99.5th percentile (equivalent to two days per year) simultaneously over an area of at least 20 km^2, allowing events to last up to 14 days. This resulted in a set of 14,400 widespread events: approximately 20 events per year, per ensemble member, per time-slice. Overall, results have shown that events are more temporally concentrated in winter in the future time-slice compared to the baseline. Distributions of event area were similar in both time-slices, but the distribution of at-site return periods showed some heavier tails in the future time-slice. Results were consistent across ensemble members, with none showing significant difference in distribution.

1 Introduction

According to the 2020 UK National Risk Register (HM Government, 2020), river flooding is one of the highest impact hazards affecting the UK. Flood prediction, and more generally flood frequency estimation, is crucial to mitigating these hazards to reduce impact. Flood frequency estimation is often carried out on a single-site basis, computing the frequency of floods at specific locations in isolation. However, the management of flood risk on a regional or national basis requires an understanding of how likely it is that multiple locations will experience floods at the same time. Widespread flooding presents a huge challenge for local communities and emergency response services and has long-lasting impacts, as demonstrated by the extensive flooding experienced in North-West England as a consequence of Storm Desmond and Storm Frank in winter 2015/2016 (Barker et al., 2016).

One approach to risk quantification is catastrophe modelling (CAT modelling), which is used in the insurance industry to assess annual average losses. CAT modelling typically makes use of three components: property data, stochastic hazard event sets and a relationship between magnitude of hazard and the expected loss for each property (Grossi and Kunreuther, 2005). The present work focuses on the second component: developing a set of widespread flood events, here characterised by river flow and the probability of exceeding that flow. Simply making use of observed widespread events typically does not provide

https://doi.org/10.5194/hess-2022-243
Preprint. Discussion started: 28 July 2022


Hydrology and Earth System Sciences
Discussions

enough data to reliably determine hazard probability. Therefore, developing a larger set of events for analysis is desirable to improve the uncertainty of risk estimates, particularly for events which have a return period (or average recurrence interval) greater than the length of observed records. For example, return periods as long as 1 in 200 years are often used as the design standard for large-scale engineering projects. This can involve making use of hydrological models driven by large ensembles of driving data from climate models (ensembles of model runs using perturbed parameter sets) over a shorter time period (Kelder et al., 2020), or through predominantly stochastic event-based models (Filipova et al., 2019).

Climate change affects flow regimes globally (Jiménez Cisneros et al., 2014), and studies suggest that flooding in the UK is likely to become (or has already become) more frequent and severe (Collet et al., 2018). The UK's Third Climate Change Risk Assessment (CCRA3) included work which analysed the changes in risk caused by possible changes in flood dynamics (Sayers et al., 2020). CCRA3 adds to the breadth of guidance that has been developed for policymakers and water managers to try and account for such changes (Reynard et al., 2017).

This paper makes use of the Grid-to-Grid hydrological model (Bell et al., 2009) and the UKCP18 Regional Projections (Met Office Hadley Centre, 2018b) to generate two sets of over 7000 hazard events for the recent past (1980-2010) and the future (2050-2080). The question of what defines a "widespread flood event" is discussed, and differences between events in terms of extent, likelihood and duration are analysed in the context of possible changes in the spatio-temporal structure of widespread events in the future. Note that, within the context of flood frequency, this paper refers to floods or flooding events, although in reality many of these will be merely high flows that do not exceed bankfull.

2 Data

2.1 Climate projections

UK Climate Projections 2018 (UKCP18) provides information on potential changes in a range of climate variables over the 21st century, via a number of different products (Murphy et al., 2018). This dataset has previously been used to analyse river flows in the UK and how they may differ in the future due to climate change (Kay 2021; Kay *et al.*, 2021).

The UKCP18 Regional Projections (Met Office Hadley Centre, 2018b) comprise a 12-member perturbed parameter ensemble (PPE) of the Hadley Centre RCM, nested in an equivalent PPE of their Global Climate Model (GCM). The ensemble covers the period December 1980 to November 2080 under an RCP8.5 emissions scenario (Riahi et al., 2011). The 12 ensemble members are numbered from 01 to 15, where 01 uses the “standard” parameterization of the Hadley Centre RCM, and ensemble members 02, 03 and 14 are not available. The rainfall and temperature used in the present work is on a 12 km spatial resolution and a daily timestep covering England, Scotland and Wales for a synthetic 360-day year (30 days per month). The data are available re-projected from the native climate model grid to a 12 km grid aligned with the GB national grid. The re-projected daily precipitation and daily minimum and maximum temperatures are used in the present work.

In some applications, bias correction is applied to the UKCP18 precipitation grids (Murphy et al., 2018), however due to the focus on the present work on extremes rather than the whole regime in general, bias correction is not applied here.

https://doi.org/10.5194/hess-2022-243
Preprint. Discussion started: 28 July 2022


Hydrology and Earth System Sciences
Discussions

3 Methods

3.1 Hydrological model

The Grid-to-Grid (G2G) hydrological model employs digital datasets to simulate the natural flow response to rainfall across the model domain. In this study, G2G was implemented as an area-wide runoff-production and flow routing model, producing outputs on a 1km grid aligned with the GB national grid (Bell et al., 2009). G2G makes use of the UK 50m Integrated Hydrological Digital Terrain Model (IHDTM; Morris and Flavin, 1990) to derive high resolution river networks and terrain information. The network-derivation scheme of Paz et al. (2006) was used to identify 1km-resolution flow directions from hydrologically-corrected 50m river networks, following Davies and Bell (2008). The routing component of G2G applies schemes that invoke the kinematic wave approximation as their basis (Bell et al., 2007a, b). In urban and suburban areas, identified through the LCM2000 spatial dataset of land-cover (Fuller et al., 2002), responsiveness is increased through the use of an enhanced routing speed and reduced soil storage, leading to a faster response to rainfall.

This application of G2G used gridded precipitation, temperature and potential evaporation provided either by observations, or from the UKCP18 Regional Projections outlined above as inputs.

3.2 Event extraction

For each RCM ensemble member, two time-slices were considered: 1980-2010 and 2050-2080, to serve as baseline and future viewpoints. Event time series were extracted using a peak-over-threshold (POT) approach as used by the NRFA (Robson and Reed, 1999). In this approach, peaks are identified as exceedances above some predetermined threshold. To improve the independence of events, they must be sufficiently far apart (based on the average time-to-peak of storm hydrographs). Additionally, consecutive events are checked to see if the minimum flow between the two peaks is less than two-thirds of both peaks, otherwise the lower peak is discarded (this process is iterated until no more events are removed).

To determine the most appropriate exceedance threshold to use at each 1km grid-square, five different percentiles of flow were investigated, ranging from five events per year to one event every 10 years on average. As a result, for each grid-square the following numbers of days were selected for each time-slice:

- 5 events per year (POT5) – 148 days per grid-square
- 2 events per year (POT2) – 60 days per grid-square
- 1 event per year (POT1) – 30 days per grid-square
- 1 event in 5 years (Q_5) – 5 days per grid-square
- 1 event per decade (Q_{10}) – 3 days per grid-square

Note this is independent of the distribution of the data due to the use of empirical percentiles rather than fixed, absolute values of flow.

To determine when widespread events occurred, different levels of extent above threshold were investigated to ensure that a good range of widespread events were captured, whilst ensuring that only events that could be described as “extreme” in some

https://doi.org/10.5194/hess-2022-243
Preprint. Discussion started: 28 July 2022


Hydrology and Earth System Sciences
Discussions

way were retained. To this end, the extent of an event was measured by the percentage of grid-squares on the river network which were simultaneously above their respective threshold values; this was considered equivalent to a grid-square being "inundated", although the river channel at this location might not be actually inundated in a physical sense. Five minimum extents were investigated: 5%, 2%, 1%, 0.5%, and 0.1%. Note that for the GB river network, 19,914 grid-squares were considered as being in the network, so an extent of 1% corresponds to ~200 km^2 of inundated grid-squares.

To select the at-site threshold and minimum extent, all the combinations above were trialled on a single ensemble member (01) for the 1980-2010 time-slice, and the number of days fulfilling both inundation criteria (at-site threshold and minimum extent) over the 30-year time-slice are shown in Table 1.

Table 1 Number of days where national inundation according to a given threshold (rows) exceeds a certain percentage (columns).

		Extent lower threshold				
# exceedences	**Daily PoE**	**5%**	**2%**	**1%**	**0.5%**	**0.1%**
5/yr	5/360	839	1510	1981	2418	3427
2/yr	2/360	353	727	1027	1340	2031
1/yr	1/360	160	401	589	826	1345
0.2/yr	1/720	25	77	144	239	444
0.1/yr	1/3600	14	35	74	117	262

The POT2 threshold and the 0.1% minimum extent were selected for the following reasons. POT2 provided a good balance between having enough exceedances to derive widespread events and keeping the threshold high enough to reasonably model the peaks-over-threshold using an extreme-value distribution. The 0.1% inundation coverage was selected to ensure that events of lesser extent that included more extreme single-point flow values were retained in the dataset. For applications in risk estimation, these events of smaller extent may occur in areas with high potential economic losses, and so are important for accurately estimating national annual damages.

With this set of parameters for inundation, the specific at-site thresholds were calculated for each grid-square under each RCM ensemble member, using the thresholds from the 1980-2010 time-slice for both present and future events. This was to allow the future events to be described in terms of present-day return periods.

At this point, the event set consisted only of single-day events, which may not truly represent widespread events in the temporal sense, owing to the way in which storms move across a region over time and the typical time taken for water to travel downstream. To correct this, multi-day events were also defined. For the selected inundation threshold (POT2), event lengths were defined as the number of consecutive days for which the extent exceeded the selected spatial limit (0.1%). For the RCM 01 ensemble member in the 1980-2010 time-slice, the distribution of event lengths is shown in Fig 1.

https://doi.org/10.5194/hess-2022-243
Preprint. Discussion started: 28 July 2022

Hydrology and Earth System Sciences
Discussions

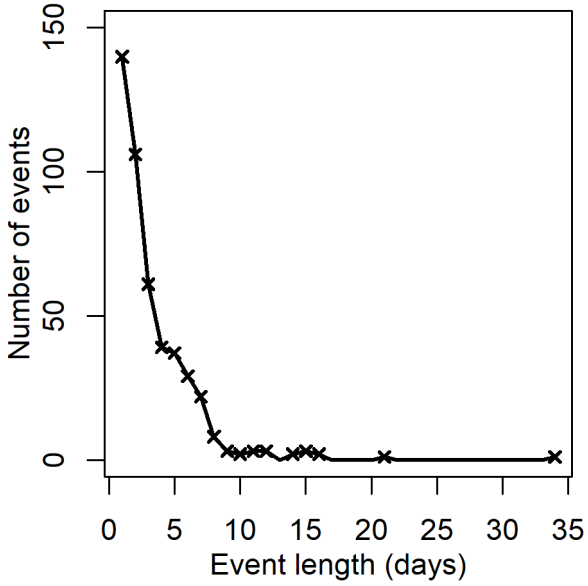

Figure 1 Number of events with different durations, based on 0.5% coverage and at-site exceedance of two days per year.

Here it can be seen that beyond seven days, there are very few events which fall under the definition above. There are some arguments that one should consider events up to 21 days (De Luca, 2017) but this may lead to a greater likelihood of two independent events of small geographical spread being recorded as a single, larger event. Such pairs (or larger groupings) of events may arise from different weather systems in, for example, the North-West and South-East of England. As a compromise therefore, events were limited to 14 days. If an event exceeded this time limit, the 14 days surrounding the day at which spatial spread was highest were retained as "the event" (six before, seven after).

To keep the events simple to interpret, multi-day events were summarised. For each grid-square, each event was summarised by the highest single-day value at that grid-square during that event. Taken nationally, this retains the maximum flow at each point over the whole region, which should capture the most extreme flows within an event, and will also be helpful for estimating upper bounds of risk associated with such events. A more in-depth investigation into multi-day events could be the focus of future work.

To assess the change in spatial extremal datasets, one can investigate whether the spatial dependence changes between time-slices; χ and $\bar{\chi}$, two measure of extremal dependance (Coles, 2001), are calculated between pairs of points. $\bar{\chi}$ describes the level of asymptotic independance between two random variables if both are above given thresholds. χ complements this: if two random variables are asymptotically dependent, this describes the strength of that dependence.

https://doi.org/10.5194/hess-2022-243
Preprint. Discussion started: 28 July 2022


Hydrology and Earth System Sciences
Discussions

3.3 Return Periods

To ensure a good fit of return periods for the most extreme events, the top 60 independent peaks were found using the peak-extraction algorithm as described in Section 3.2. For values over the threshold, a Generalised Pareto distribution (GPa) was used with distribution function

$$F_{GPA}(x) = 1 - \left(1 + \frac{\kappa(x-u)}{\alpha}\right)^{\frac{1}{\kappa}} = P[Flow > x | Flow > u]$$

with threshold u, scale parameter $\alpha > 0$ and shape parameter $-1 \leq \kappa \leq 1$. This was fitted to the series of independent peaks over the threshold to give a modelled daily probability of exceedance. To smoothly transition between the empirical distribution for the lower flows and the GPa distribution the following expression was used, as described in Towe et al., (2016) to more appropriately describe probability of non-exceedance for all values of flow:

$$F(x) = \begin{cases} F_{GPA}(x) P[x > u] \; if \; x > u \\ \mathrm{F_{EMP}}(x) \; if x \leq u \end{cases}$$

where F_{EMP} is the empirical cumulative distribution function, u is the flow threshold at a specific location, and $P[x > u] = 2/360$, since this investigation uses the POT2 threshold defined in Section 3.2.

Probabilities of exceedance (PoE) were determined using daily data, and so to convert from a daily PoE to a more widely-used annual PoE, a Poisson approximation was used based on a 360-day year:

$$p_{ANNUAL} = 1 - \exp(-360\, p_{DAILY})$$

In the rest of this work, plots are presented using annual probabilities of exceedance. For reference, if $p_{DAILY} = 2/360$, then $p_{ANNUAL} \approx 0.865$. Due to the limits of using 30-year time-slices of data, return periods are capped at 1000 years since the uncertainty on exceedance probabilities is very high for the most infrequent events.

4 Results

Fig 2 shows four example events extracted from the 1980-2010 time-slice from RCM ensemble member 01, with return periods described in years. The coloured extent of an event was restricted to those points with a daily probability of exceedance of less than 2/360.

https://doi.org/10.5194/hess-2022-243
Preprint. Discussion started: 28 July 2022

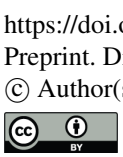

Hydrology and Earth System Sciences
Discussions

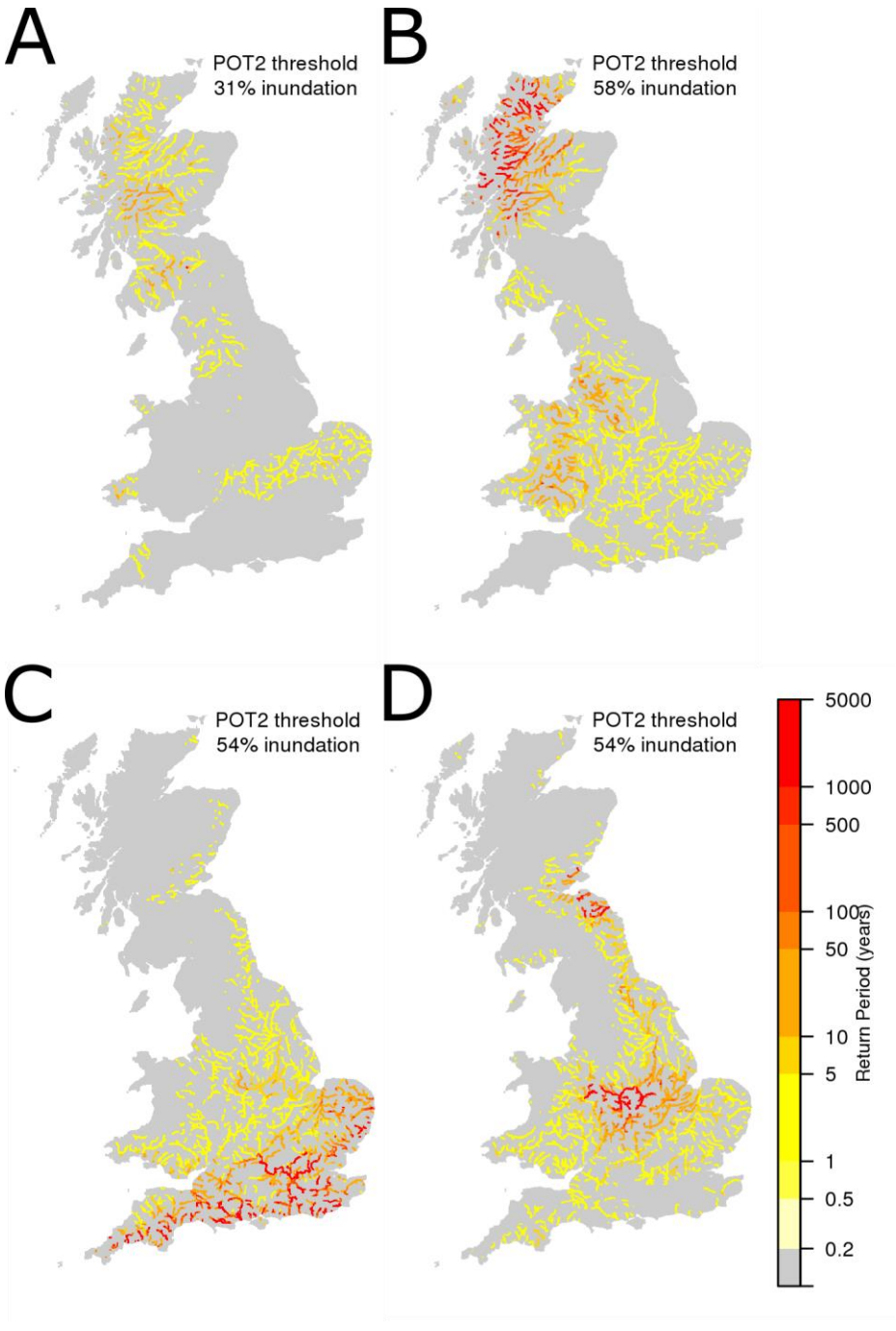

Figure 2 Example events from 1981-2010 time-slice from a single RCM ensemble member, showing return period in years.

On the whole, the events are spatially contiguous, although the event in Fig 2a does suggest that some number of potentially simultaneous but independent events are captured; this may be due to two separate events happening on consecutive days due to the method of event length determination. This suggests that a more sophisticated form of event delineation could improve

https://doi.org/10.5194/hess-2022-243
Preprint. Discussion started: 28 July 2022


Hydrology and Earth System Sciences
Discussions

the process. Also, the example events suggest that return period is highly peaked around one location and quickly tapers off away from the "epicentre". These are four of the largest events in the 1980-2010 time-slice, and show a broad range of different events covering Scotland, southern England and central England, with key patches of very extreme flow in Fig 2b, Fig 2c and Fig 2d, whereas Fig 2a shows a widespread but less severe event (in terms of return period of flow).

In this paper, analysis focuses on the differences between past and future and across space, though differences between the RCM ensemble members should be mentioned. Fig 3(a, c) shows that the event areas are fairly consistent between ensemble members for both time-slices, although ensemble members 07 and 08 shows a slightly more uniform distribution of events across log(Area), and ensemble member 11 shows a slightly higher number of small events. For return periods (Fig 3b, Fig 3d), the overall distribution is fairly consistent across ensemble members and time-slices. Ensemble member 01 shows the greatest difference between the 1980-2010 and 2050-2080 time-slices, although all the ensemble members show a slightly flatter distribution of return periods in the 2050-2080 time-slice. In the rest of this section, the event sets from all ensemble members are combined and given equal weighting.

https://doi.org/10.5194/hess-2022-243
Preprint. Discussion started: 28 July 2022

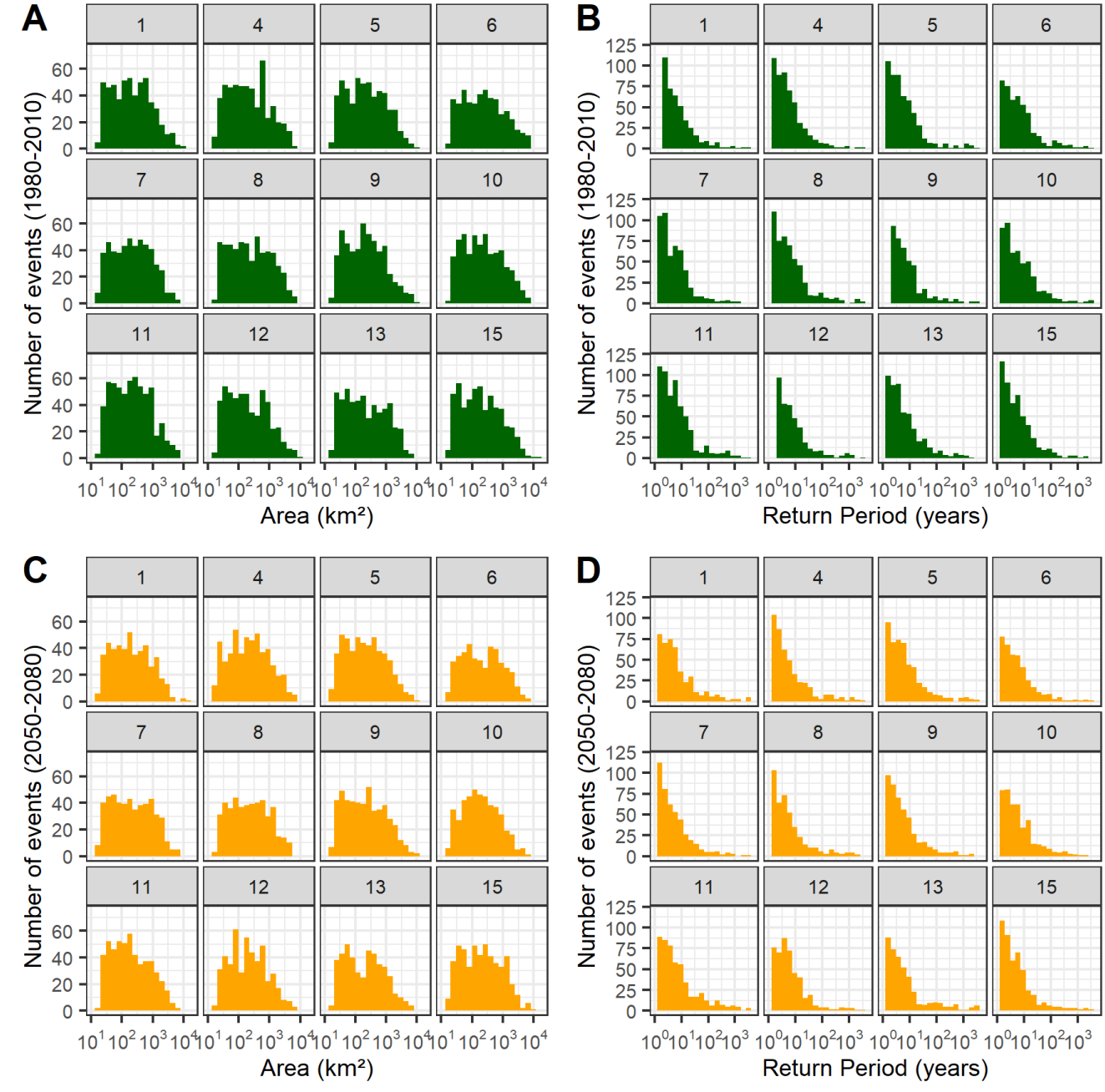

Figure 3 Histograms showing distribution of event area and return period, split across time-slices and ensemble members.

Taking the union of events extracted from all the ensemble members, changes in extent and duration can be examined. Figure 4 highlights the changes in the number of widespread between the two time-slices, subdivided by season. The figure shows overall more widespread events in the future (7553) than in the 1980-2010 time-slice (7225 events). However, in the months

https://doi.org/10.5194/hess-2022-243
Preprint. Discussion started: 28 July 2022

Hydrology and Earth System Sciences
Discussions

of March to August, and particularly in June to August, one sees fewer widespread events in the future time-slice. This may suggest a shift to more widespread flooding in winter, and drier summers overall, which lines up with the literature (Murphy et al., 2019). Alternatively, this may instead be linked to a change in the size of flooding events in the future in summer events which, in the UK, are typically linked to short-duration, intense summer storms. It may be the case that these intense storms may become smaller in extent, below this paper's definition of "widespread". However, Chen et al. (2021) suggests, using the UKCP18 Local projections (which uses convection-permitting models rather than RCMs), that convective storms in future may cover a greater area. Thus future work could look more specifically at differences in the methods which could cause these differences.

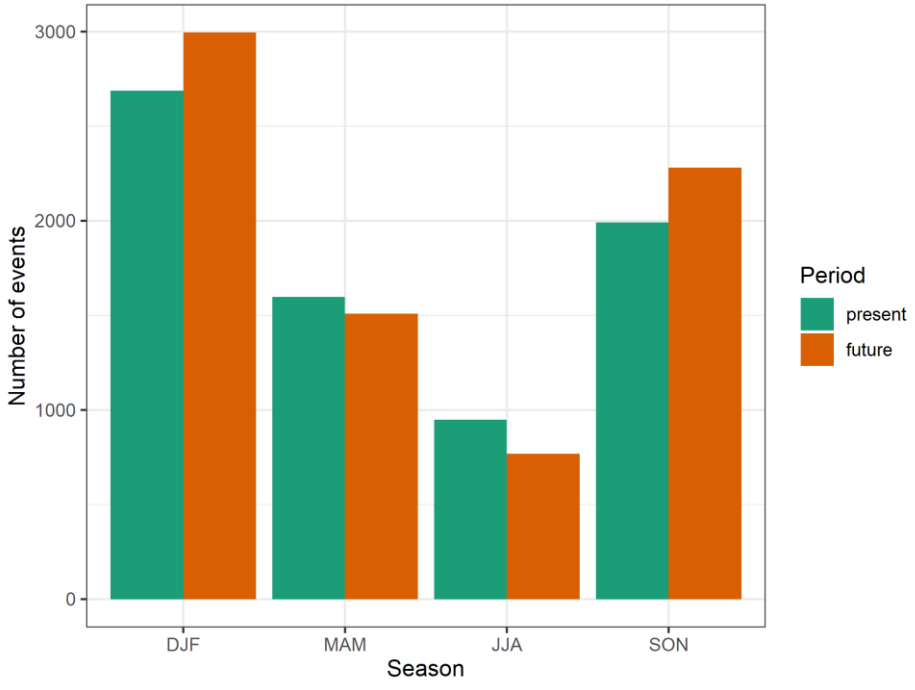

Figure 4 Number of widespread events, summed across ensemble members, split by season and time-slice.

In terms of event duration, Fig 5shows how this varies by season and time-slice, and how that is linked to return period. The figure suggests that duration and return period are somewhat correlated, in that the longest duration events are very unlikely to have a low return period (i.e. to occur frequently). However, there are a number of events which are of short duration but high return period. As one might expect, events are shorter in summer (JJA), with very few summer events extending longer than 5 days. In the future time-slice, event duration seems to be slightly shorter on average, and this is more pronounced in summer (JJA) and autumn (SON). The events with the highest return periods are in autumn (SON) and winter (DJF), in both time-slices, though the distribution of return periods in the future has heavier tails (note the return period axis is on a logarithmic scale).

https://doi.org/10.5194/hess-2022-243
Preprint. Discussion started: 28 July 2022

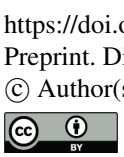

Hydrology and Earth System Sciences
Discussions

Figure 6shows how area and peak return period vary by season in the two time-slices. As one might expect, there is a correlation between area and peak pointwise return period across both time-slices. The changes between the two time-slices are subtle, but there is an overall trend towards an increase in the range of peak return period. The extent of widespread events appears to stay consistent between the 1980-2010 and 2050-2080 time-slices, with a possible slight reduction in extent of the largest
205 events in the future summer. On the right of some panels (future winter and autumn) is a set of events with a peak return period of at least 1000 years. Although extreme, Tawn et al. (2019) point out that, within the observed AMAX series, the chance of a 100-year return period event occuring somewhere within a set of 916 gauging stations in England and Wales is approximately 78%, and so over a gridded dataset of more points, and with more events, the observation of these extremely rare events is not so surprising. Also, due to the probability distributions used, a small change in flow in the upper tail of the distribution can
210 lead to a large change in return period (when the shape parameter κ is positive, which is the case for most of the UK (Griffin et al., 2019)).

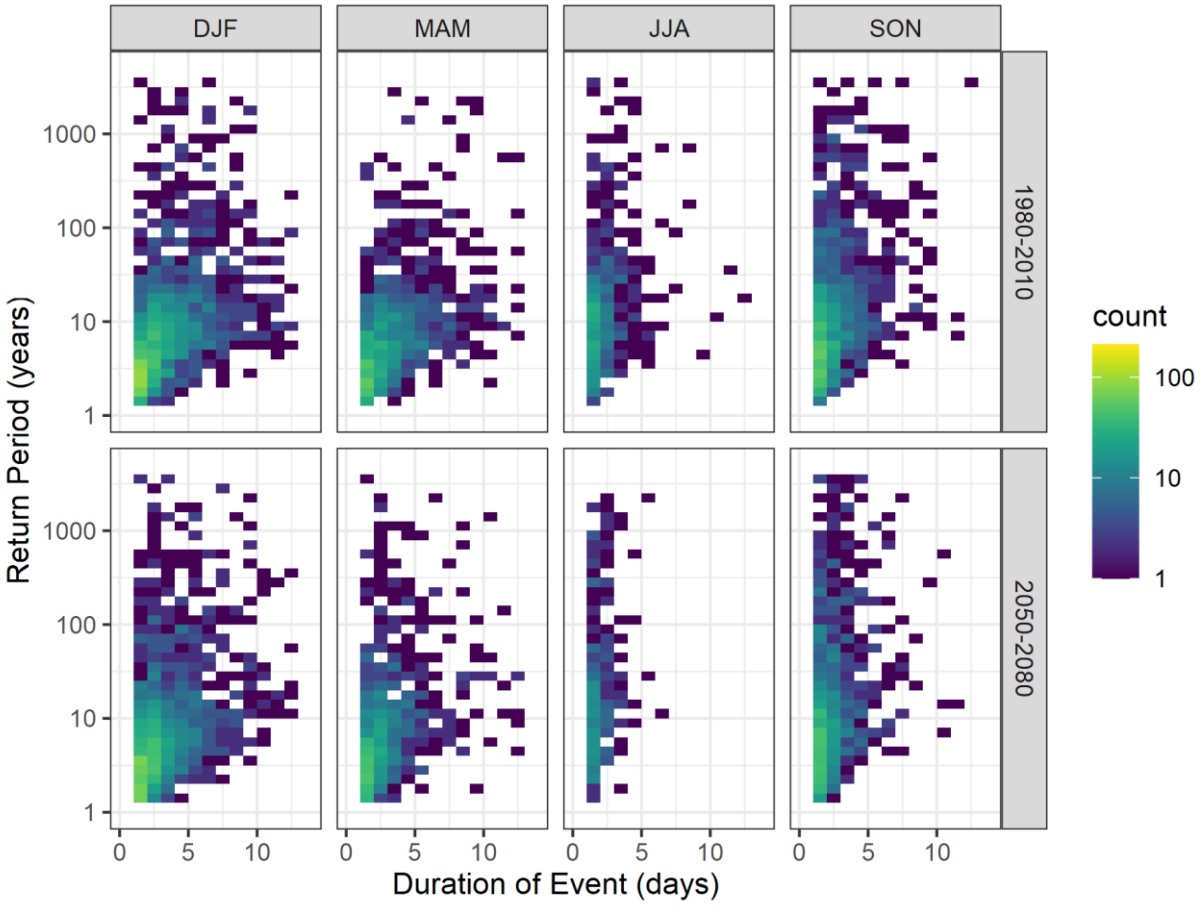

Figure 5 Heatmaps showing joint distribution of return period and event duration, summed across ensemble members, split by season and time-slice.

https://doi.org/10.5194/hess-2022-243
Preprint. Discussion started: 28 July 2022

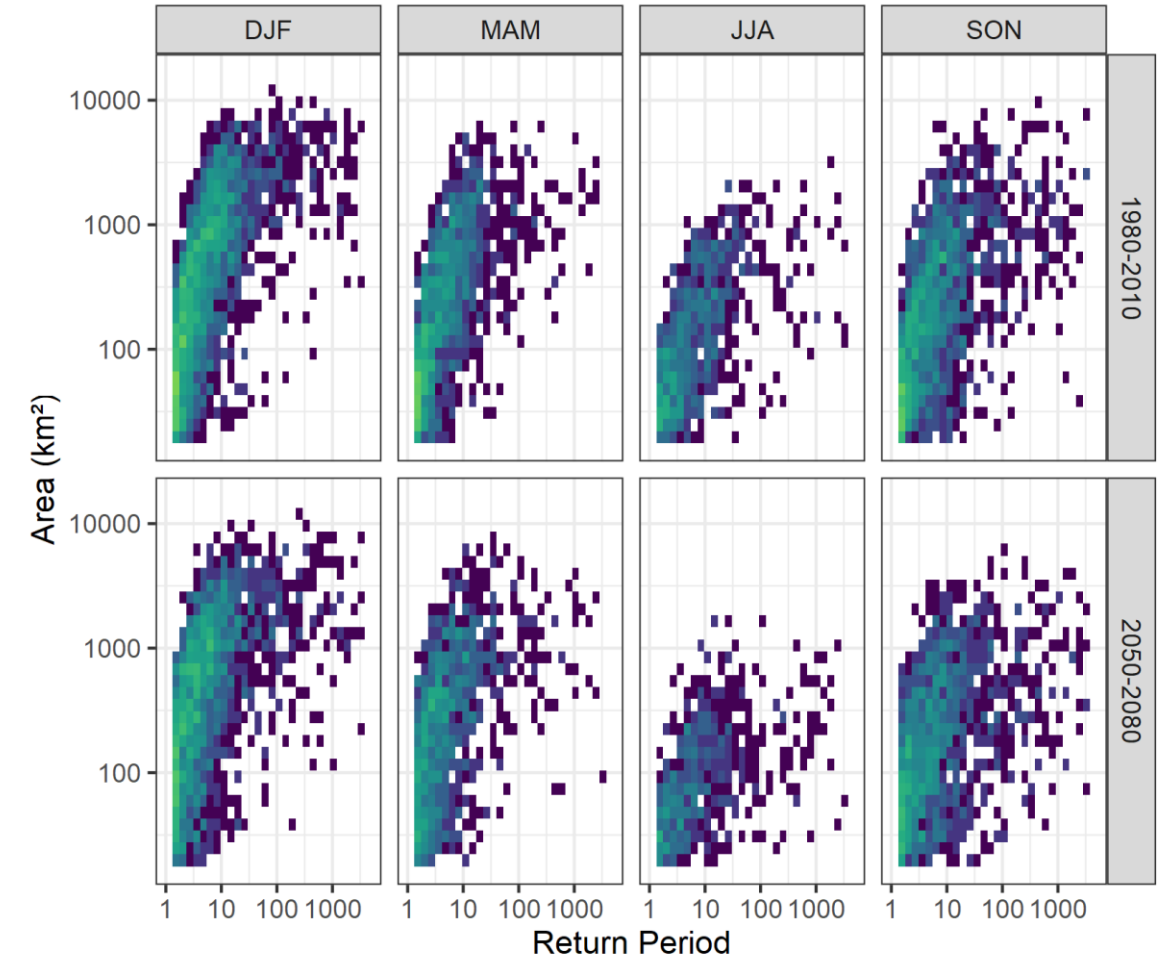

Figure 6 Heatmaps showing distribution of events with different areas and return periods, split by time-slice and season, summed across all ensemble members.

Figure 7 shows how dependence varies between pairs of points across the river network. Here aymptotic dependence appears to have a limit of around 120km (χ is only shown for pairs of locations for which the upper bound of a bootstrapped uncertainty bound of $\bar{\chi}$ exceeds 0.99). The figure suggests that dependence generally decreases as distance increases. There seems to be little change in dependence between the two time-slices, although the asymptotic dependence appears to extend slightly further in the future time-slice. If the events are subdivided by season, subtle differences can be observed (Fig 8). Overall, spring and summershows less asymptotic dependence (lower values of χ and $\bar{\chi}$) than autumn and winter. Also, the 50% contour for $\bar{\chi}$ is longer in spring than summer in both time-slices, suggesting that the variance in $\bar{\chi}$ exhibits seasonal variation. Between present and future, as forFig 7, the differences are marginal, but both χ and $\bar{\chi}$ show smaller 50% contours in autumn, suggesting reducing variation in asymptotic dependence in this season. For other percentile contours, patterns are very similar and follow the shapes ofFig 7.

https://doi.org/10.5194/hess-2022-243
Preprint. Discussion started: 28 July 2022

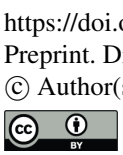

Hydrology and Earth System Sciences
Discussions

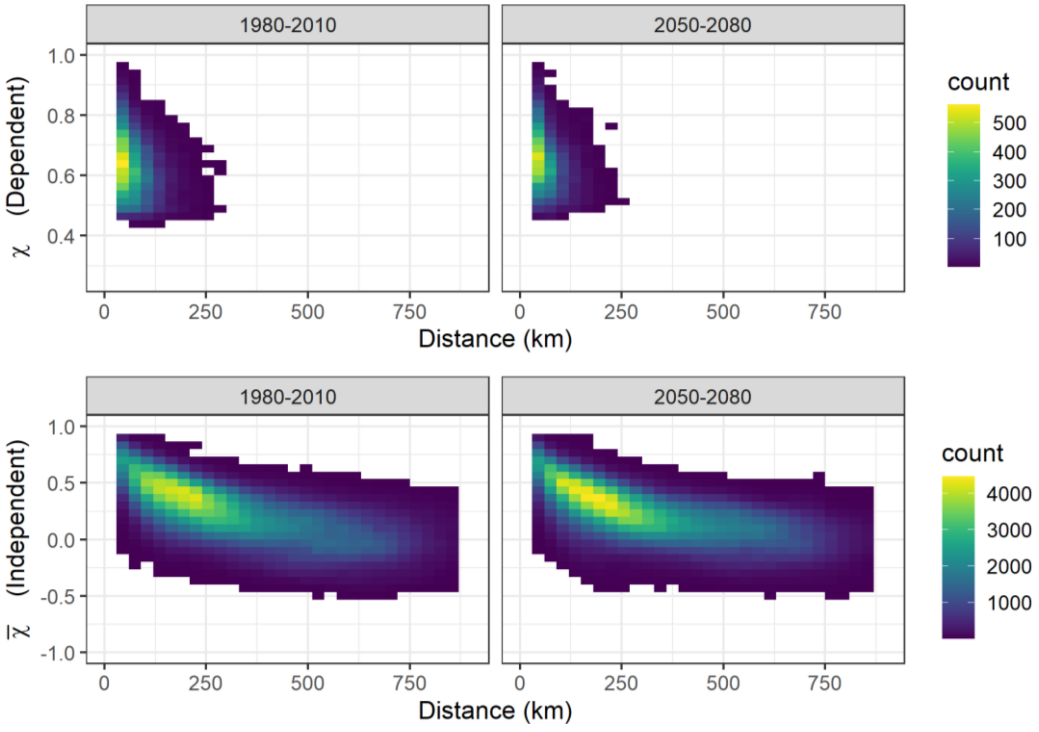

Figure 7 Heatmaps showing asymptotic dependence for 100 000 random pairs of points on the river network. χ is only shown for pairs of locations which are asymptotically dependent based on $\bar{\chi} > 0.99$.

https://doi.org/10.5194/hess-2022-243
Preprint. Discussion started: 28 July 2022

Hydrology and Earth System Sciences
Discussions

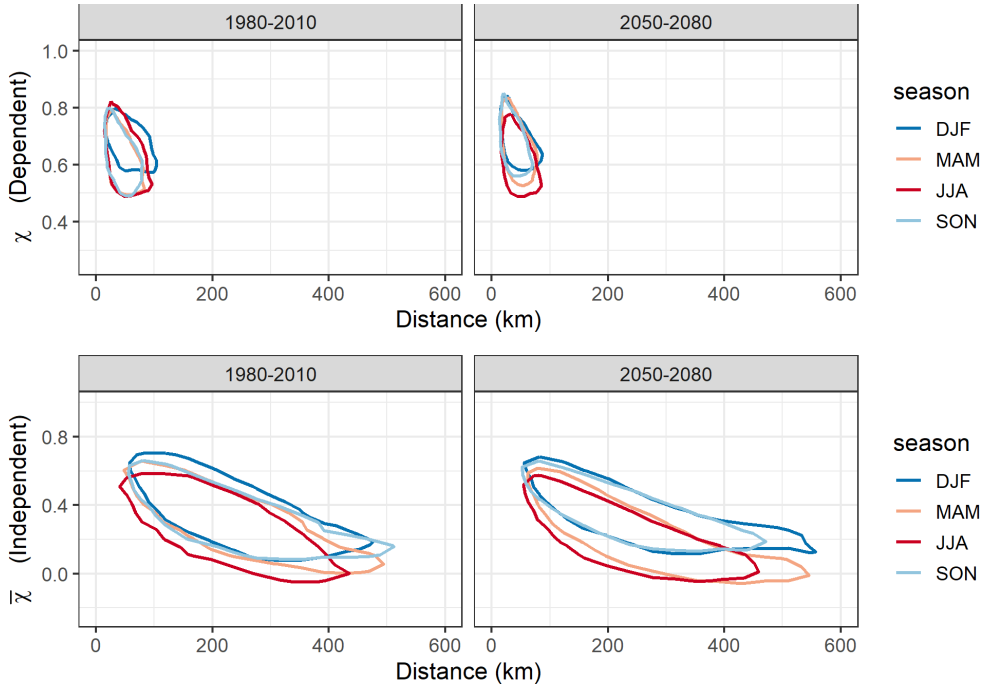

Figure 8 Contour showing asymptotic dependence for 100 000 random pairs of points on the river network. Contours show smallest area that contains 50% of point-pairs, split by season and time-slice. χ and $\overline{\chi}$ as in Figure 7

5 Discussion and Conclusions

This paper has used UKCP18 Regional Projections and the Grid-to-Grid (G2G) hydrological model to generate a set of widespread flood events to investigate changes in spatial structure of river flooding in mainland Great Britain between the 1990s and 2060s. In summary, the number of widespread events (based on a POT2 threshold derived from 1980-2010 data) was found to increase in total in the future time-slice, but was slightly lower in the future for spring and summer (March-August) events. The typical spatial extent of events was found to be fairly consistent between time-slices, but summer (June-August) events appeared smaller in the future across all return periods. Event duration decreased on average in all seasons between the two time-slices. This pattern was the same across all RCM ensemble members. A pairwise analysis suggested that inundated locations were asymptotically independent beyond a radius of around 120 km, but the distribution of dependence was slightly less concentrated in the future.

On the whole, the results suggest an increase in seasonality in widespread flood events, with more widespread flooding in winter, and possibly a shift towards smaller intense flooding in spring and summer. However, this approach cannot distinguish between flooding drivers such as convective storms, and so it is difficult to say what could cause such a change in the model. As mentioned above, the use of convection-permitting models (Chen et al., 2020) may prove useful in drawing out such differences and highlighting likely changes in flooding drivers.

https://doi.org/10.5194/hess-2022-243
Preprint. Discussion started: 28 July 2022


Hydrology and Earth System Sciences
Discussions

This paper and the data generated therein forms the basis for a wider scheme of work generating extreme flooding events for risk analysis, which is the subject of a number of subsequent papers: Griffin et al., (2022b) discussing statistical methods to generate large numbers of plausible widespread events with long return periods and Sayers et al., (in prep) on applying the event sets to risk analysis through catastrophe modelling methods.

Several potentially simultaneous but disjoint events were captured in the event sets, which may be due to capturing two consecutive or overlapping events due to the method of event length determination. Further work could look at more sophisticated methods of event identification, and look at describing or separating simultaneous or temporally-overlapping events. This work focuses on fluvial flooding but surface water flooding is also a large factor in estimating economic losses due to flooding. It would be of interest to use the Grid-to-Grid model including surface water (Rudd et al., 2020) applied to the framework of this paper to see if the different types of flooding will change in different ways over time.

Data availability

Peak flow data freely available from UK National River Flow Archive (nrfa.ceh.ac.uk). UKCP18 data available from Met Office under and Open Government Licence. Event set can be found at the EIDC (Griffin et al., 2022a)

Author Contributions

ES and PS managed the project, AK and VB ran the hydrological modelling, AG ran the event extraction and summary, and performed the statistical analysis. All authors assisted in writing and editing the manuscript.

Acknowledgements

Funding for the project was provided through the UK Climate Resilience Programme supported by UK Research and Innovation and the UK Met Office.

References

Barker, L., Hannaford, J., Muchan, K., Turner, S. and Parry, S. (2016). The winter 2015/2016 floods in the UK: a hydrological appraisal. Weather, 71: 324-333. doi:10.1002/wea.2822

Bell, V.A., Kay, A.L., Jones, R.G., Moore, R.J. (2007a). Development of a high-resolution grid-based river flow model for use with regional climate model output. Hydrol. Earth Syst. Sci. 11 (1), 532–549. doi:10.5194/hess-11-532-2007

Bell, V.A., Kay, A.L., Jones, R.G., Moore, R.J. (2007b). Use of a grid-based hydrological model and regional climate model outputs to assess changing flood risk. Int. J. Climatol. 27, 1657–1671. doi:10.1002/joc.1539

275 Bell V.A., Kay A.L., Jones R.G. et al. (2009). Use of soil data in a grid-based hydrological model to estimate spatial variation in changing flood risk across the UK. J. Hydrol. 377(3–4): 335–350. doi:10.1016/j.jhydrol.2009.08.031Chen Y, Paschalis A, Kendon E, Kim D, Onof C (2020). Changing spatial structure of summer heavy rainfall, using convection-permitting ensemble. Geophysical Research Letters, 48, e2020GL090903. doi: 10.1029/2020GL090903.

280 Collet, L., Harrigan, S., Prudhomme, C., Formetta, G., & Beevers, L. (2018). Future hot-spots for hydro-hazards in Great Britain: A probabilistic assessment. Hydrology and Earth System Sciences Discussions, 1–22. doi:10.5194/hess-2018-274

Davies, H., Bell, V. (2008). Assessment of methods for extracting low resolution river networks from high resolution digital data. Hydrol. Sci. J. 54 (1), 17–28. doi:10.1623/hysj.54.1.17

De Luca, P., Hillier, J. K., Wilby, R. L., Quinn, N. W., Harrigan, S. (2017). Extreme multi-basin flooding linked with extra-
285 tropical cyclones. Environmental Research Letters, 12(11), 114009. doi:10.1088/1748-9326/aa868e

Environment Agency (2011). The risk of widespread flooding – Capturing spatial patterns in flood risk from rivers and coasts. Science Report SC060088/R3. Bristol.

Filipova, V., Lawrence, D., Skaugen, T. (2019) A stochastic event-based approach for flood estimation in catchments with mixed rainfall and snowmelt flood regimes. Natural Hazards and Earth System Sciences, 19(1), 1-18. doi:10.5194/nhess-19-
290 1-2019

Fuller, R.M., Smith, G.M., Sanderson, J.M., Hill, R.A., Thomson, A.G. (2002). The UK Land Cover Map 2000: Construction of a Parcel-Based Vector Map from Satellite Images, The Cartographic Journal, 39:1, 15-25, doi:10.1179/caj.2002.39.1.15

Griffin, A.; Kay, A.; Bell, V.; Stewart, E.J.; Sayer, P.; Carr, S. (2022a). Peak flow and probability of exceedance data for Grid-to-Grid modelled widespread flooding events across mainland GB from 1980-2010 and 2050-2080. NERC EDS
295 Environmental Information Data Centre. doi:10.5285/26ce15dd-f994-40e0-8a09-5f257cc1f2ab

Griffin, A., Kay A., Stewart, E., Sayers, P., Carr, S. (2022b). Spatially coherent statistical simulation of widespread flooding events under climate change. *Submitted to Hydrology Research.*

Grossi, P., & Kunreuther, H. (2005) Catastrophe Modeling: A New Approach to Managing Risk (Vol. 25). Springer Science & Business Media.

300 Guillod, B. P., Jones, R. G., Dadson, S. J., Coxon, G., Bussi, G., Freer, J., Kay, A. L., Massey, N. R., Sparrow, S. N., Wallom, D. C. H., Allen, M. R., Hall, J. W. (2018). A large set of potential past, present and future hydro-meteorological time series for the UK. Hydrology and Earth System Sciences, 22, pp.611–634. doi:10.5194/hess-22-611-2018

Hosking, J., Wallis, J. (1997). Regional Frequency Analysis: An Approach Based on L-Moments. Cambridge: Cambridge University Press. doi:10.1017/CBO9780511529443

305 Hough, M. N., Jones, R. J. A. (1997). The United Kingdom Meteorological Office rainfall and evaporation calculation system: MORECS version 2.0-an overview. Hydrology and Earth System Sciences, 1(2), pp.227-239. doi:10.5194/hess-1-227-1997

HM Government, 2020. National Risk Register: 2020 edition. Cabinet Office: London.

https://doi.org/10.5194/hess-2022-243
Preprint. Discussion started: 28 July 2022

Jones, M. R., Blenkinsop, S., Fowler, H. J., Kilsby, C. G. (2014). Objective classification of extreme rainfall regions for the UK and updated estimates of trends in regional extreme rainfall. International Journal of Climatology, 34(3), pp.751-765. doi:10.1002/joc.3720

Kay A.L. (2021) Simulation of river flow in Britain under climate change: Baseline performance and future seasonal changes. Hydrological Processes. 35, e14137. doi:10.1002/hyp.14137

Kay, A. L., Griffin, A., Rudd, A. C., Chapman, R. M., Bell, V. A., Arnell, N. W. (2021). Climate change effects on indicators of high and low river flow across Great Britain. Advances in Water Resources, 151, 103909. doi:10.1016/j.advwatres.2021.103909

Kelder, T., Müller, M., Slater, L. J., Marjoribanks, T. I., Wilby, R. L., Prudhomme, C., Bohlinger, P., Ferranti, L., Nipen, T. (2020). Using UNSEEN trends to detect decadal changes in 100-year precipitation extremes. npj Climate and Atmospheric Science, 3(1), 47. doi:10.1038/s41612-020-00149-4

Met Office, Hollis, D (2019). Had UK-Grid Gridded Climate Observations on a 1km grid over the UK, v1.0.0.0 (1862–2017). Centre for Environmental Data Analysis, November 2019. doi:10.5285/2a62652a4fe6412693123dd6328f6dc8.

Morris, D.G. and Flavin, R.W. (1990). A digital terrain model for hydrology. Proc 4th International Symposium on Spatial Data Handling. Vol 1 Jul 23-27, Zürich, pp 250-262.

Murphy J, Harris G, Sexton D, Kendon E, Bett P, Clark R and Yamazaki K (2019). UKCP18 land projections: science report. Met Office: Exeter. www.metoffice.gov.uk/pub/data/weather/uk/UKCP18/science-reports/UKCP18-land-report.pdf [accessed Nov 2021]

Murphy, J. M., Harris, G. R. (2018). UKCP18 Land Projections: Science Report. Met Office Hadley Centre, Exeter.

National River Flow Archive (NRFA), 2020. https://nrfa.ceh.ac.uk [accessed Sep 2021]

Osborn, T.J. and Hulme M. (2002). Evidence for trends in heavy rainfall events over the UK. Phil. Trans. R. Soc. A. 360, pp.1313–1325. doi:10.1098/rsta.2002.1002

Sayers, P.B., Horritt, M., Carr, S., Kay, A., Mauz, J., Lamb R., and Penning-Rowsell E. (2020). Third UK Climate Change Risk Assessment (CCRA3): Future flood risk. Published by Committee on Climate Change, London.

Rudd, A.C., Kay, A.L., Wells, S.C., Aldridge, T., Cole, S.J., Kendon, E.J. and Stewart, E.J. (2020). Investigating potential future changes in surface water flooding hazard and impact. Hydrological Processes, 34, 139-149, doi:10.1002/hyp.13572.

Robson, A. J., & Reed, D. W. (1999). Statistical procedures for flood frequency estimation. In Flood Estimation Handbook (Vol. 3, p. 338). Institute of Hydrology.

Tanguy, M.; Dixon, H.; Prosdocimi, I.; Morris, D.G.; Keller, V.D.J. (2019). Gridded estimates of daily and monthly areal rainfall for the United Kingdom (1890-2017) [CEH-GEAR]. NERC Environmental Information Data Centre. doi:10.5285/ee9ab43d-a4fe-4e73-afd5-cd4fc4c82556

Tawn, J.A., Towe, R.P., Eastoe, E., Lamb, R. (2018). Modelling the clustering of extreme events for short-term risk assessment. Spatial Statistics, *28*, pp.39–58. doi:10.1016/j.spasta.2018.04.007

https://doi.org/10.5194/hess-2022-243
Preprint. Discussion started: 28 July 2022

Hydrology and Earth System Sciences
Discussions

Towe, R.P., Tawn, J.A., Lamb, R., Sherlock, C. (2019). Model-based inference of conditional extreme value distributions with hydrological applications. Environmetrics. 2019; 30:e2575. doi:10.1002/env.2575